Elasto-plastic 3D FE analysis of the seismic behavior in culvert longitudinal direction of three-hinge type of precast arch culverts

AUTHOR(S):

Miyazaki, Y.; Sawamura, Y.; Kishida, K.; Kimura, M.

Elasto-plastic 3D FE analysis of the seismic behavior in culvert longitudinal direction of three-hinge type of precast arch culverts

Y. Miyazaki[a]*, Y. Sawamura[a], K. Kishida[b] and M. Kimura[a]

[a] *Department of Civil and Earth Resources Engineering, Kyoto University, Kyoto, Japan*
[b] *Department of Urban Management, Kyoto University, Kyoto, Japan*
* miyazaki.yusuke.73x@st.kyoto-u.ac.jp (*sawamura.yasuo.6c@kyoto-u.ac.jp, kishida.kiyoshi.3r@kyoto-u.ac.jp, kimura.makoto.8r@kyoto-u.ac.jp)*

Abstract

The Great East Japan earthquake (11 March 2011) caused loss of serviceability on many three-hinge type of precast arch culverts, which indicated importance of clarification of its damage mechanism. However, there is no effective seismic evaluation method available in the current design criteria of the precast arch culverts for the observed damages correlated with the inertial force to the longitudinal direction. On the other hand, our research group has conducted the series of dynamic centrifuge tests on the precast arch culverts to observe the seismic behavior in culvert longitudinal direction. As the results, the seismic behavior in the longitudinal direction of the precast arch culverts is controlled by their longitudinal, structural connectivity and confining stress of the culverts from the embankment. In short, in a numerical analysis, the longitudinal seismic behavior of the precast arch culverts should be governed by these effects due to longitudinal, structural connection and overburden of culverts.

Therefore, in the present study, 3D elasto-plastic finite element analyses for three-hinge type of precast arch culvert were conducted to develop a new evaluation method for the longitudinal, seismic performance of the precast arch culverts. In these analyses, the structural connection is modeled by non-linear spring element and the slip and separation between the culvert and the soil is modeled by joint element. From the analysis results, the patterns of the deformation of the culverts and the embankment and axial force behavior of the structural connections due to the various embankment shape can be evaluated.

Keywords: Elasto-plastic 3D FE analysis, seismic behavior in culvert longitudinal direction, three-hinge type of precast arch culverts

1. Introduction

Three-hinge type of precast arch culvert (Fig. 1) is one of the precast style culverts which enables labor saving and high-quality control construction by using precast concrete members. As shown in Fig. 1, this hinged arch culvert is a statically determinate structure due to the three hinge structures at arch crown and arch foots respectively. On the other hand, the hinged arch culvert is likely to collapse due to the deviation of hinge, which has emphasized the interest of the seismic stability of the hinge structure; e.g. Sawamura et al., (2016) aimed to clarify the damage morphology and the ultimate state of the three-hinged arch culvert through the large table shaking tests on 1/5 model of three-hinged arch culvert. As results, the deviation of hinge is unlikely to occur in advance of the failure of arch members even after the strong earthquake which caused more than 7 % of shear strain of ground.

On the other hand, the Great East Japan earthquake (11 March 2011) caused critical damages to 9 old-type of three-hinged arch culverts (refer to Fig. 1) with the loss of their serviceability. Fig. 2 shows the schematic figure of one of the damaged culverts described by Abe and Nakamura (2014). The figure was described based on the observation from the inside of the culvert. The damages to the culverts such as the continuous tip of the arch crown and the water leakages between the arch members seems to be correlated with the inertial force in culvert longitudinal direction. Especially, the old type of the three-hinged arch culvert is weak in the longitudinal structural connectivity without the concrete beam, which seems to cause the larger longitudinal displacements of the arch members.

Although the damage related with culvert longitudinal earthquake was reported, there is no consideration of the longitudinal seismic performance and few related academic researches.

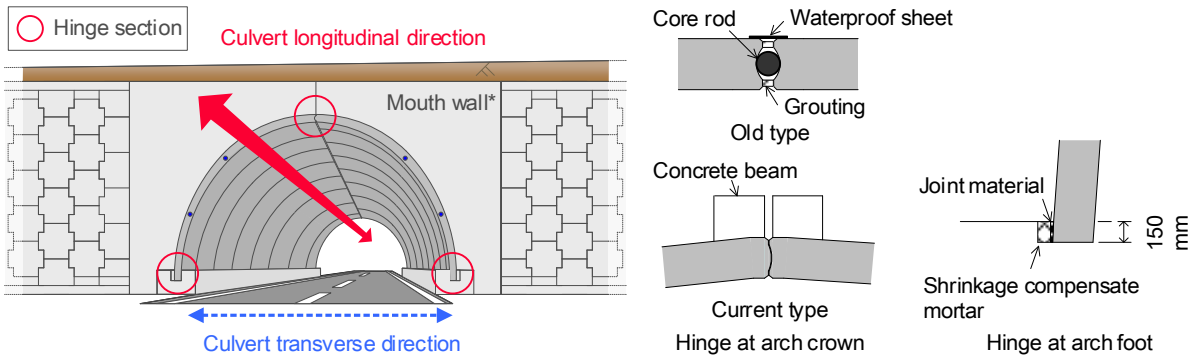

Fig. 1. Structural outline of three-hinge type of precast arch culverts.

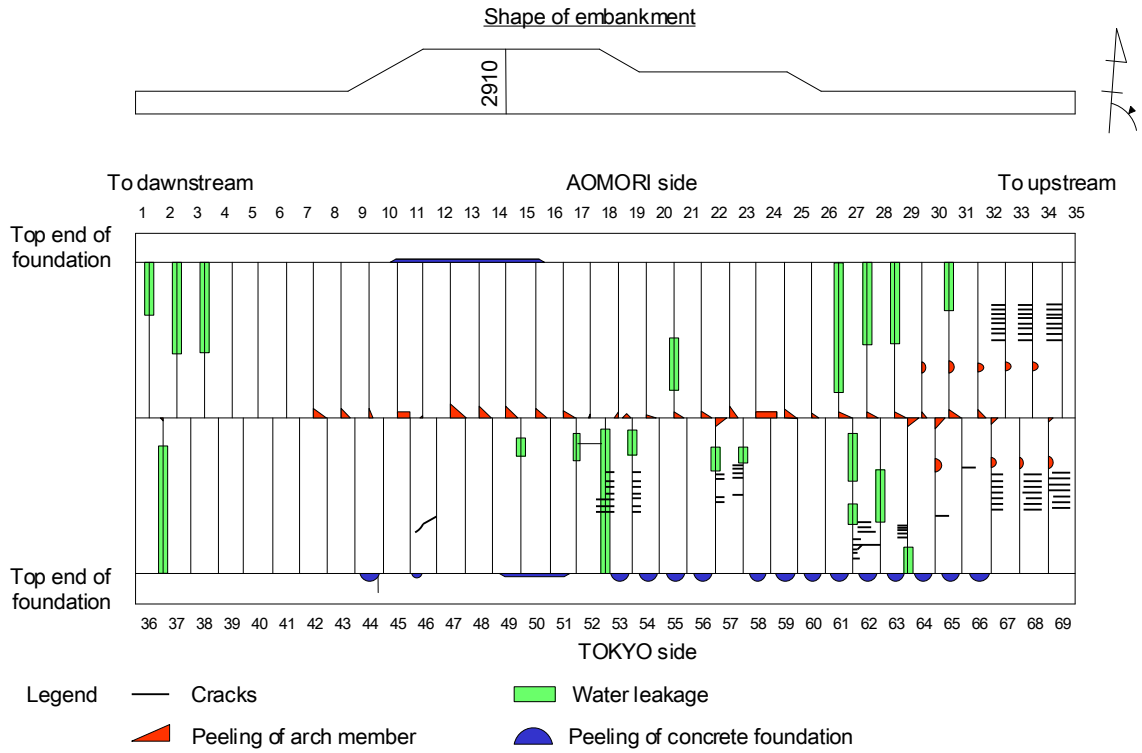

Fig. 2. The schematic drawing of three-hinge type of precast arch culverts after the Great East Japan earthquake reported by Abe and Nakamura (2014).

Therefore, our research group has respectively investigated the influence of the structural connectivity of and the embankment patterns of the culverts on the longitudinal seismic behavior. As the experimental results, the structural connectivity dominants the displacements of the culverts; separating the culverts allows the independent movement of each of the culverts, which causes the aperture of the culverts after the earthquake (Miyazaki et al., 2017). The embankment patterns strictly control the response acceleration of the culverts; less overburden of the culverts gives less integration of the seismic behavior between the culverts and the embankment (Miyazaki et al., 2018).

The present study aims to develop a new evaluation method of the seismic performance in the precast arch culverts considering the knowledges based on the above dynamic centrifuge tests. In advance of the development, the 3D elasto-plastic finite element analysis manipulated by DBLEAVES (Ye et al., 2007) was conducted for the longitudinal seismic behavior of the three-hinged arch culverts. In this paper, how the input wave of culvert longitudinal direction would affect on the damage to the culverts was discussed.

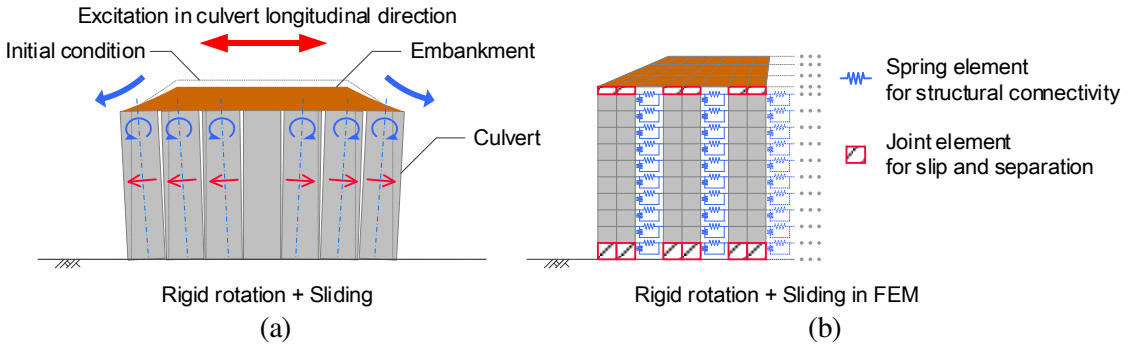

Fig. 3. Deformation mode of culverts due to seismic wave in culvert longitudinal direction. (a) observed deformation mode in the experiment (Miyazaki et al, 2017a) and (b) expression in finite element method.

2. Outline of numerical analysis

2.1 FEM modeling for seismic behavior in culvert longitudinal direction

Fig. 3 shows the deformation mode of culvert with embankment due to culvert longitudinal direction about the observed deformation in the dynamic centrifuge test (Miyazaki et al., 2017) and the FEM modeling. From Fig. 3 (a), the longitudinal seismic behavior of the culverts can be explained with rigid rotation of and sliding of culvert with embankment deformation. Therefore, in this FEM analysis, the rigid rotation of the culverts was controlled with nonlinear spring element arranged at the structural connection of culverts and the separation and slip were controlled with joint element arranged at the interface of culvert and soil as shown in the figures. The embankment deformation was modeled by an elasto-plastic constitutive model.

2.2 FEM mesh and analysis case

Fig. 4, 5 shows the analysis meshes. This analysis study focused on 20 m long of the three-hinged arch culverts on the ground foundation of 5.0 m thickness. The precast arch culverts generally are used as an underpass of road embankment, so that the distance of the culverts was decided to satisfy the available distance for two-lane road of the embankment crown. As shown in the figures, Case-1 was the 1.0 m overburden of the culverts and Case-2 was the 5.0 m overburden of the culverts.

2.3 Mechanical properties of soil

The mechanical properties of soil were based on Edosaki sand. Foundation ground was modeled by an elastic model whose stiffness equals to 30 in N value of SPT and embankment was modeled by Cyclic mobility model (Zhang et al., 2007). This constitutive model was developed for simple modeling without change of parameters of stress-induced anisotropic in soil due to soil density, over consolidation ratio, soil structure given by natural accumulating process and various stress histories. These profiles were decided by isotropic consolidation test and triaxial compression test for Edosaki sand (Sawamura et al., 2016). Table 1 shows the parameters of embankment. The initial stress of foundation ground was decided by the self-weight analysis and that of embankment was assumed as K_0 state.

2.4 Interface of arch members

Fig. 6 shows the modeling of soil-structure and structure-structure interface about arch elements and Table 1 shows the material properties of culvert. From the figures, joint element was arranged on the interface between arch culvert and soil for modeling slip and separation. In longitudinal structural connection of the arch members, nonlinear spring element was arranged. Hinge of arch crown was modeled with nonlinear spring elements between elements of arch crowns and hinge of arch foot was modeled with joint element between elements of arch foot and foundation.

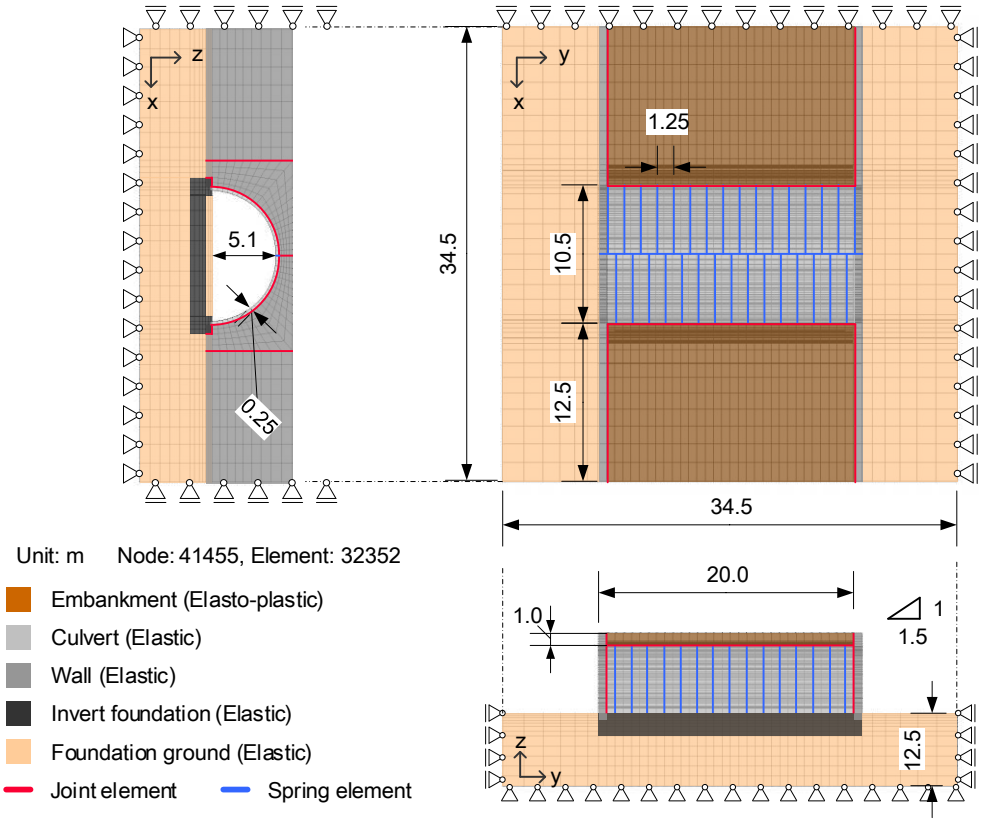

Fig. 4. Analysis mesh in Case-1

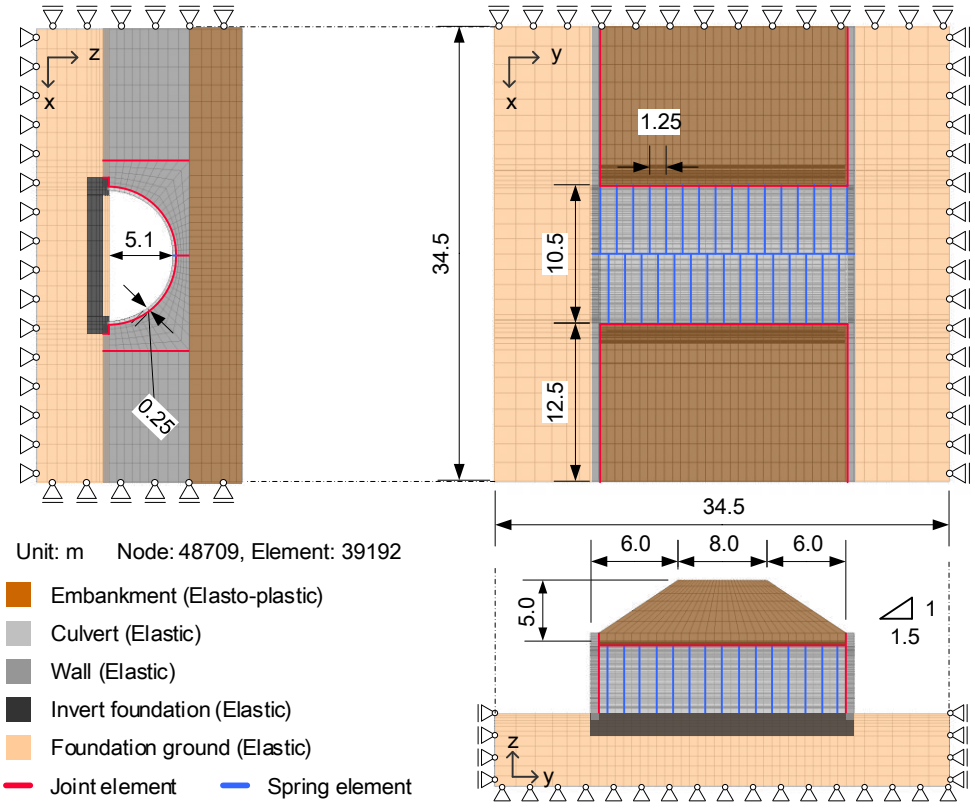

Fig. 5. Analysis mesh in Case-2

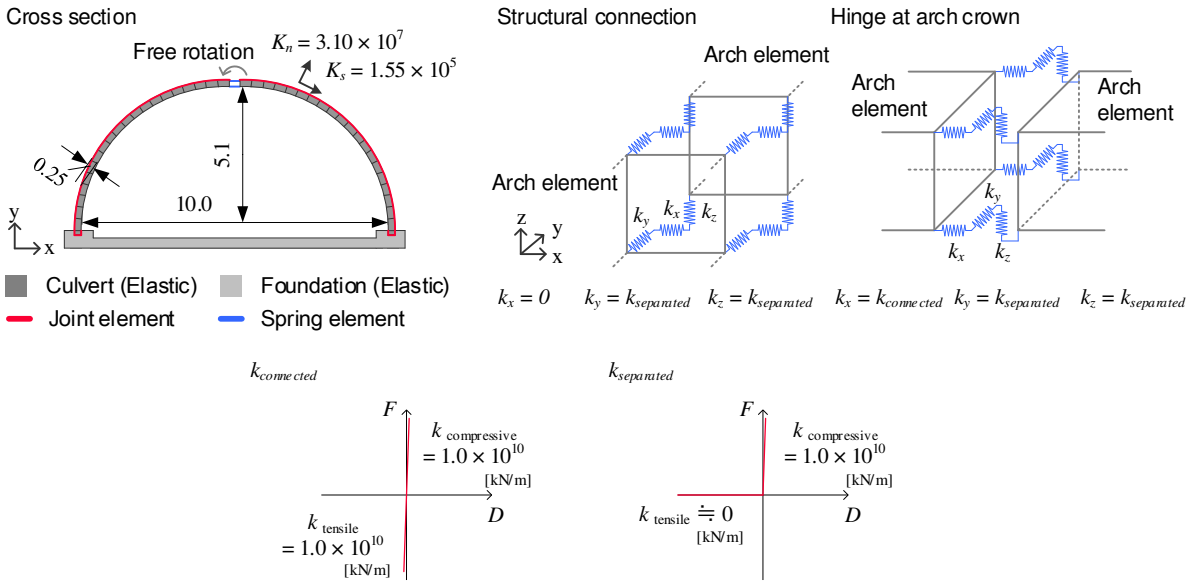

Fig. 6. Soil-structure interface and structur-structure interface of arch element.

In this analysis, to express the aperture and water leakage reported in the Great East Japan earthquake, the arch members were modeled in the separated condition without the structural connection. Therefore, the spring constant was controlled to equal zero of tensile stiffness at contactless and enough larger stiffness than concrete at contact. The hinge at arch crown was modeled by zero of rotating stiffness and the hinges at arch foots were modeled by joint element as shown in the figures. The parameters for the joint element was decided by the direct shear test for mortar and Toyoura sand (Sawamura et al., 2016).

2.5 Model of mouth wall

As shown in Fig. 1, the mouth wall of three-hinged arch culvert is constructed as a perpendicular wall of embankment generally with reinforced earth wall. In the past experiments (e.g. Miyazaki et al., 2018), the unity of embankment and mouth wall modeled as reinforced earth wall was not spoiled during the repeated input of the longitudinal earthquake.

Therefore, in this analysis, considering the unity of embankment and mouth wall, the mouth wall was modeled as an elastic, concrete without reinforcing member. Joint element was arranged at the interface between soil and wall and the shear stiffness was set in enough larger stiffness to express the integral deformation of embankment with mouth wall.

2.6 Input wave

For the input wave, a sin wave with 1 Hz, 3 cycles and 300 gal of magnitude (Fig. 7) was used to observe the simple seismic behavior. The wave was input on the bottom of ground foundation in culvert longitudinal direction. The time interval of calculation was 0.001 second and the time integration was based on a Newmark-β method ($\beta = 1/4$, $\gamma = 1/2$).

3. Dynamic analysis results

3.1 Seismic behavior in culvert longitudinal direction

Fig. 8 shows the time history of response acceleration in Y direction at arch crown. From the figures, in Case-1 and Case-2, some vibration appeared in the response acceleration at Pos 1. As mentioned later, the shift of the arch member Pos 1 belonging to occurred. This arch member had unstable behavior due to repeated collision, which caused the vibration of the response acceleration at Pos 1. Here, simply the magnitude of the response acceleration is compared in Case-1 and Case-2.

Table 1. Properties of concrete

Young's modulus E_a	[kN/m^2]	3.10×10^7
Unit weight γ	[kN/m^3]	24.5
Poisson's ratio ν	—	0.20
Damping ratio h	—	0.02

Table 2. Soil properties for embankment

Principal stress ratio at critical state $Rcs = (\sigma 1 / \sigma 3)_{CS(comp.)}$	4.0
Compression index λ	0.08194
Swelling index κ	0.01014
$N = e_{NC}$ at p = 98 kPa & q = 0 kPa	1.06
Poisson's ratio ν_e	0.276
Degradation parameter of overconsolidation state m	0.02
Degradation parameter of structure a	0.65
Evolution parameter of anisotropy b_r	0.4
Wet unit weight (kN/m^3) γ_t	17.738
Initial degree of structure R^*_0	0.1491 ~ 0.1584
Initial anisotropy ζ_0	0.5

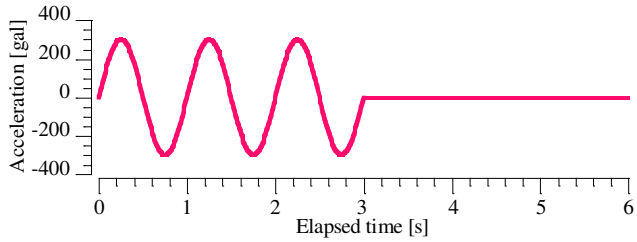

Fig. 7. Input wave is sin wave with 1 Hz, 3 cycles and 300 gal magnitude.

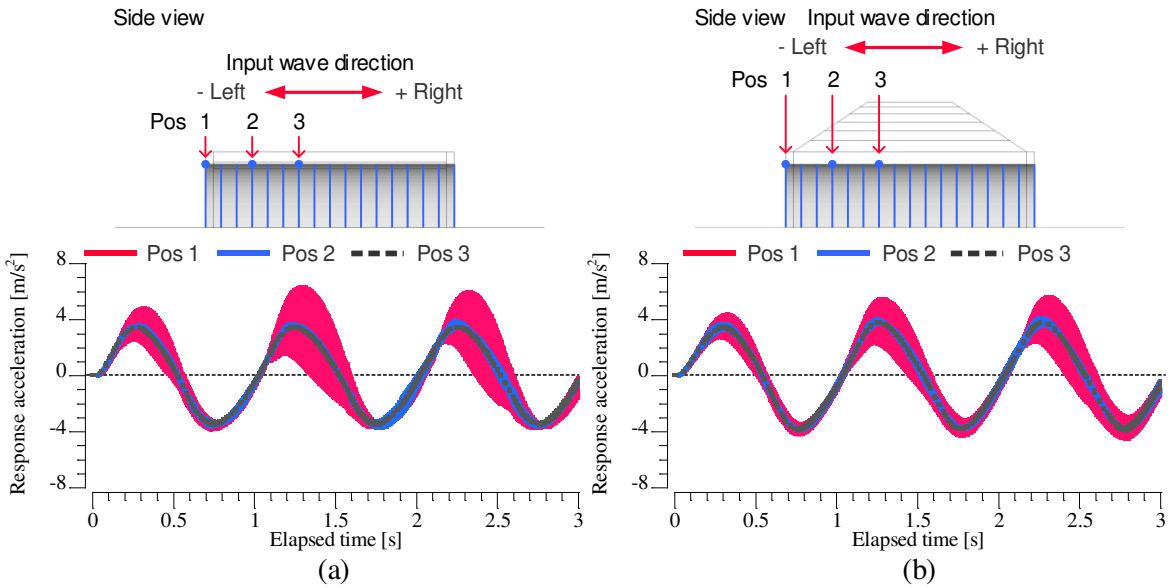

Fig. 8. Time history of response acceleration at arch crown in Y direction: (a) Case-1and (b) Case-2.

From the figures, both Case-1 and Case-2 showed the amplified magnitude at Pos 1 where located at the mouth of culvert. Especially in Case-1 which has smaller overburden, the difference of magnitude due to the position was clear. Hence, maximum response accelerations at half of all arch members were plotted in Fig. 9. From the figure, in both Case-1 and Case-2 the maximum response acceleration got increased at the closer position to the mouth of culvert. Additionally, in Case-1, the amplification of acceleration at the arch members near the mouth of culvert got larger compared with Case-2. This is because the smaller overburden of culvert at mouth of culvert gave the smaller confining stress acting on culverts from surrounding ground. As a result, the response acceleration of arch members at mouth of culvert seems to get amplified. This tendency of response acceleration was observed in the dynamic centrifuge tests considering patterns of overburden (Miyazaki et al., 2018).

This amplified response acceleration of arch members influenced on the aperture of culverts and the unique embankment deformation. Fig. 10, 11 respectively shows the culverts and the embankment after excitation. From the figure of the deformed embankment, compared with Case-2, Case-1 showed the different displacement-mode between area of culvert and are of no culvert. The settlement of the embankment was larger on the culverts and the horizontal displacement of mouth of culvert was

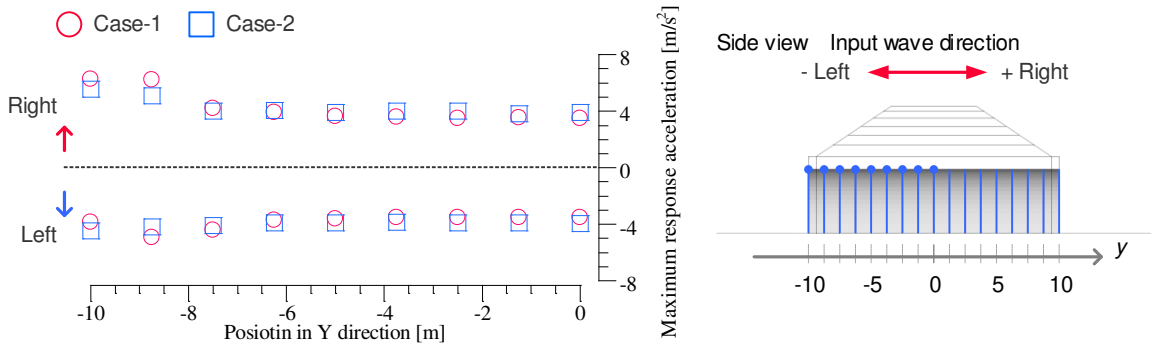

Fig. 9. Maximum response acceleration in Y direction at arch crown of each arch-members.

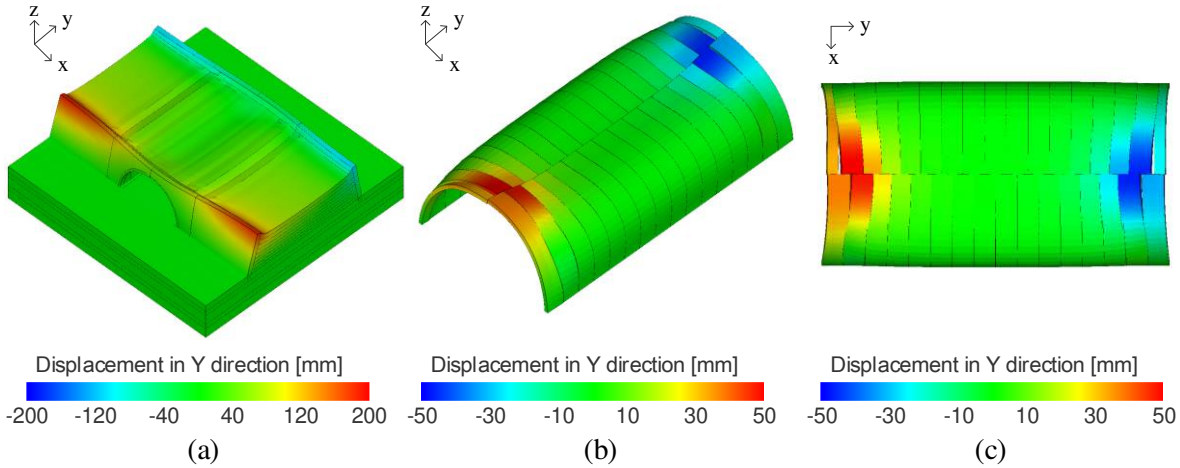

Fig. 10. Heat map of displacement in Case-1 after excitation: (a) displacements in Y direction of culvert with embankment and (b) displacements in Y direction of culvert from oblique view and (c) from top view. The displacement output is enlarged by 10 times as the original one.

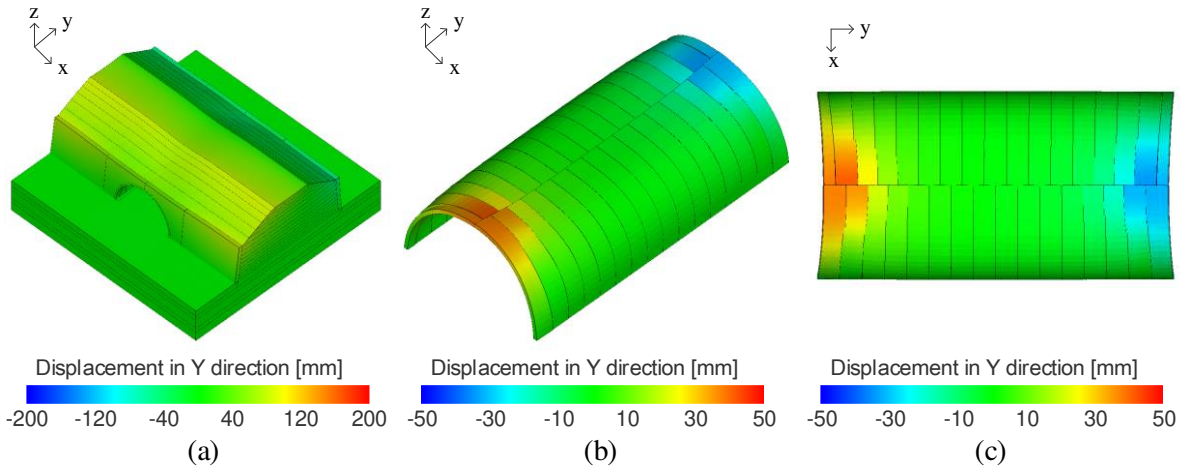

Fig. 11. Heat map of displacement in Case-2 after excitation: (a) displacements in Y direction of culvert with embankment and (b) displacements in Y direction of culvert from oblique view and (c) from top view. The displacement output is enlarged by 10 times as the original one.

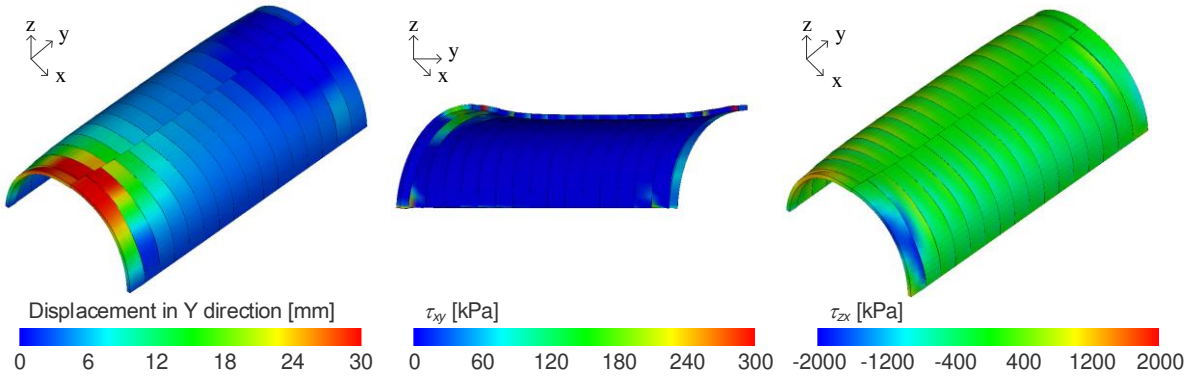

Fig. 12. Heat map of Case-1 at t = 2.0 s: (a) displacements in Y direction of culvert, (b) τ_{xy} on arch crown of cross section and (c) τ_{zx} on culvert from oblique view.

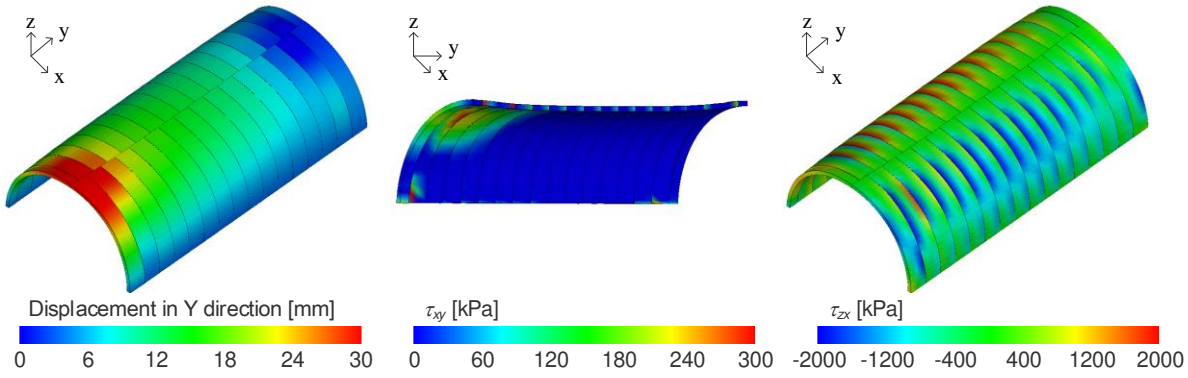

Fig. 13. Heat map of Case-2 at t = 2.0 s: (a) displacements in Y direction of culvert, (b) τ_{xy} on arch crown of cross section and (c) τ_{zx} on culvert from oblique view.

smaller near the culverts. About the figure of culvert deformation, in Case-1, there were shift in vertical direction and aperture of the arch member near the mouth of culvert. In Case-2, there was no observed clear aperture like Case-1 although the shift of the arch member at mouth of culvert was observed.

From the above results, displacements of arch members are likely to occur in the location under small overburden where confining stress from embankment is weak. Thereby, the aperture of culverts and the water leakage due to the aperture will occur in the arch members with small overburden.

3.2 Stress condition of three-hinged arch culvert

In the Great East Japan earthquake, the characteristic damages to the culverts such as the continuous tips of the arch crowns and the bending cracks occurred (Fig. 2). Therefore, about Case-1 and Case-2, the response displacements and stress condition during excitation were summarized in Fig. 12, 13. In the figure, the output was shown at t = 2.0 s when clear embankment deformation began to occur.

From the figures, in Case-1, the displacement in Y direction occurred mainly in the mouth of culvert. However, in Case-1, the displacements occurred from the mouth of culvert to the center of culvert. Here, τ_{xy} is the stress to cause the shear deformation in culvert longitudinal direction. When focusing on the arch crown, τ_{xy} seems to be correlated with the displacements in Y direction in both cases. In Case-1, stress concentration occurred on the arch crowns near the mouth of culvert. On the other hand, in Case-2, the stress concentration on the arch crowns continuously occurred along the depth direction. Moreover, the magnitude of the stress was larger in Case-2 than that in Case-1.

Here, τ_{zx} is the stress to cause the shear deformation in culvert transverse direction. Although τ_{xy} was concentrated on the arch shoulders in both cases, the area of stress concentration was different.

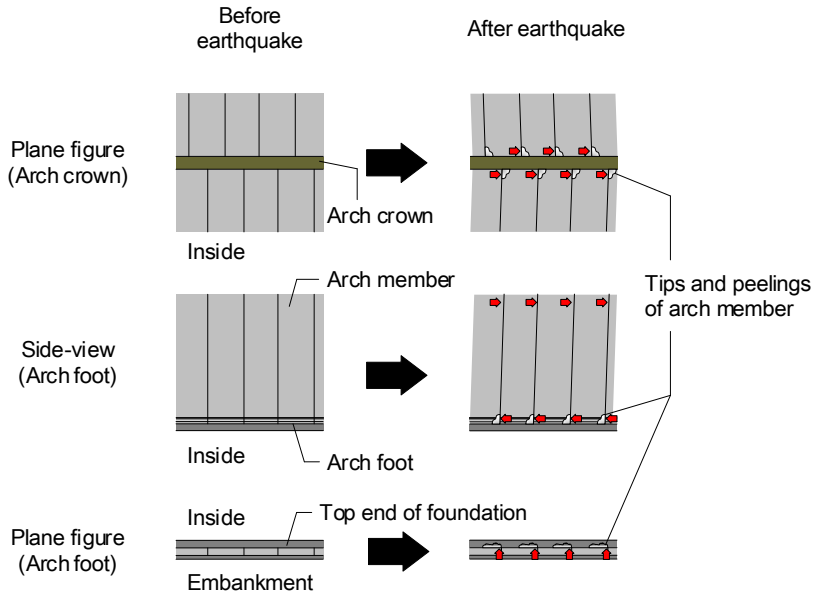

Fig. 14. Mechanism of damage to arch members the Great East Japan earthquake assumed by Abe and Nakamura (2014)

The stress concentration occurred on the arch members near the mouth of culvert in Case-1 but on most of the arch members in Case-2. This is because the embankment deformation due to culvert longitudinal earthquake observed in Fig. 10, 11 caused the shear stress of the culvert cross section. Especially in Case-2, the larger shear stress along the excitation direction on each of arch members, which caused the displacement of the arch members. The difference between the are of the shear stress concentration appeared as confining stress of culverts from embankment due to the difference of overburden in Case-1 and Case-2.

Abe and Nakamura (2014) assumed the damage mechanism of the arch members observed in the Great East Japan earthquake as shown in Fig.14. According to the figure, torsion of the arch members occurred due to earthquake and the arch members were knocked against each other, which caused the regular damages to the arch members. Compared with the analysis results, the earthquake in culvert longitudinal direction reproduce the continuous concentration of shear stress on the arch crowns described in Fig. 13(b), which seems to correspond to the damage mechanism of the regular tips of the arch crown.

4. Conclusions

In the present analyses, the seismic behavior in culvert longitudinal direction of the three-hinged arch culverts without the longitudinal structural connection were conducted by using nonlinear spring element through FEM. The input wave was sin wave with 1 Hz, 3 waves and 300gal magnitude. The obtained results are shown below.

1) The difference of overburden appears as a difference of confining stress acting on culverts. Three-hinged arch culverts with small overburden is likely to suffer the damage related with the displacements of the arch members such as aperture of arch members. On the other hand, the culverts with large overburden is likely to suffer the damages to the arch members themselves due to the increase of shear stress dependent on overburden thickness.
2) The seismic wave in culvert longitudinal direction causes the concentration of the longitudinal shear stress on arch crown. The embankment deformation due to the longitudinal seismic wave increases the shear stress of arch cross section on arch shoulder. As a result, each of stress concentration will cause the damage to the arch crown and arch shoulder.

Acknowledgements

This work was supported by the RESEARCH FOUNDATION ON DISASTER PREVENTION OF EXPRESS HIGHWAY BY NEXCO-AFFILIATED COMPANIES.

References

[1] Abe, T. and Nakamura, M. (2014) *The use of and the caution in the application of the culvert constructed by large pre-cast element in the expressway construction*, The Foundation Engineering & Equipment, Vol. 42, No. 4, pp. 8-11. (in Japanese)
[2] Sawamura, Y., Ishihara, H., Kishida, K. and Kimura, M. (2016) Experimental Study on Damage Morphology and Critical State of Three-hinge Precast Arch Culvert through Shaking Table Tests, Procedia Engineering, Advances in Transportation Geotechnics III, Vol. 143, pp. 522-529.
[3] Miyazaki, Y., Sawamura, Y., Kishida, K. and Kimura, M. et al. (2017) Evaluation of dynamic behavior of embankment with precast arch culverts considering connecting condition of culverts in culvert longitudinal direction, Japanese Ge-otechnical Society Special Publication, Vol. 5, No. 2, pp. 95-100.
[4] Miyazaki, Y., Sawamura, Y., Kishida, K. and Kimura, M. et al. (2018) Dynamic behavior of three-hinge type precast arch culverts installed in embankment with asymmetrical overburden in culvert longitudinal direction, Proc. of the 9th International Conference on Physical Modelling in Geotechnics, pp.915-920, London, United Kingdom, 2018-7.
[5] Ye, B., Ye, G., Zhang, F. and Yashima, A. (2007). Experiment and numerical simulation of repeated liquefaction-consolidation of sand, Soils and Foundations, Vol. 47, No. 3, pp.547-558, 2007.
[6] Zhang, F., Ye, B., Noda, T., Nakano, M. and Nakai, K. (2007) Explanation of cyclic mobility of soils: approach by stress-induced anisotropy, Soils and Foundations, 47(4), pp.547-558.